GRIDLESS CYLINDRICAL MIRROR ENERGY ANALYZER FOR ELECTRON SPECTROSCOPY

Shugayeva T.Zh.[1], Spivak-Lavrov I.F.[1], Amantaeva A.Sh.[1]
[1]K. Zhubanov Aktobe Regional University, Aktobe, Kazakhstan

tlektes.tleubaeva@gmail.com

Abstract. A two-electrode cylindrical mirror energy analyzer of charged particles is proposed and calculated. It has a high luminosity due to the axisymmetric field distribution and second-order focusing in the detector plane. Charged particles are introduced into and removed from the analyzer without using grids through an opening in the end electrodes, where the field is practically absent. The electrostatic field of the analyzer is calculated analytically using the methods of the theory of functions of a complex variable. Numerical integration of differential equations of motion and the Monte Carlo method are used to model the behavior of charged particle beams. Analyzer variants with high dispersion and luminosity are calculated.

Key words: cylindrical energy analyzers of charged particles, axisymmetric electron mirrors, gridless electron mirrors.

INTRODUCTION

At present, one of the main research methods in the field of solid state physics is electron spectroscopy. energy analyzers based on fields of cylindrical and two-dimensional mirrors have become widely used as analyzing devices. cylindrical mirror energy analyzers have high dispersion and luminosity due to the rotational symmetry of the field and the presence of second-order focusing in the detector plane. [1-4].

The main disadvantage of currently used energy analyzers based on cylindrical and two-dimensional mirror fields is the use of fine-structured grids for introducing particles into the analyzer and removing them from the analyzer. The blurring of the potential barrier on the grids limits the analytical capabilities of such devices. Therefore, the development of highly efficient gridless energy analyzers of charged particles with simple electrode geometry is an urgent task of physical electronics.

The cylindrical mirror analyzer with closed ends (CMACE) is considered in [5]. Input and output of charged particles in the analyzer is carried out through a grid system, which is its main drawback. In the present work, the input and output of particles is carried out through holes in the ends of the analyzer, where the field is practically absent, which allows to significantly improve its characteristics. In [5], an analytical expression is given for the axisymmetric potential describing the analyzer field. This expression is obtained by the standard method of separating variables in the form of an expansion in a series of Bessel functions. However, it is inconvenient to use these expressions for numerical calculation of particle trajectories due to poor convergence of the series. In [6], another method for calculating the field of axisymmetric systems is proposed, which is used in the present work.

1. CALCULATION OF THE ANALYZER FIELD

In the case of axisymmetric systems, the electrostatic field potential φ in cylindrical coordinates ρ, ψ, z depends only on variables ρ, z and satisfies the Laplace equation. Moving to dimensionless variables using the relations:

Journal of Physics: Conference Series **2984** (2025) 012030 doi:10.1088/1742-6596/2984/1/012030

$$\eta = \ln \frac{\rho}{R}, \qquad \zeta = \frac{z}{R}, \tag{1}$$

we obtain the following equation for the potential $\varphi\,(\eta,\,\zeta)$:

$$e^{-2\eta}\,\frac{\partial^2\varphi}{\partial\eta^2} + \frac{\partial^2\varphi}{\partial\zeta^2} = 0\,. \tag{2}$$

It should be noted that in the region $\rho \cong R$ variable $\eta \cong 0$ and potential $\varphi\,(\eta,\,\zeta)$ satisfies the two-dimensional Laplace equation. We will look for the potential $\varphi\,(\eta,\,\varsigma)$ as a sum of two terms

$$\varphi\,(\eta,\,\zeta) = \varphi^{(0)}(\eta,\,\zeta) + \varphi^{(1)}(\eta,\,\zeta)\,. \tag{3}$$

Here $\varphi^{(0)}(\eta,\,\varsigma)$ – harmonic potential satisfying the two-dimensional Laplace equation:

$$\frac{\partial^2\varphi^{(0)}}{\partial\eta^2} + \frac{\partial^2\varphi^{(0)}}{\partial\zeta^2} = 0 \tag{4}$$

and given boundary conditions. Using the methods of the CVFT it can be found in closed form. Then the second term $\varphi^{(1)}(\eta,\,\varsigma)$ satisfies the zero Dirichlet boundary conditions and is a solution to the following inhomogeneous equation:

$$e^{-2\eta}\,\frac{\partial^2\varphi^{(1)}}{\partial\eta^2} + \frac{\partial^2\varphi^{(1)}}{\partial\zeta^2} = \left(1 - e^{-2\eta}\right)\frac{\partial^2\varphi^{(0)}}{\partial\eta^2}\,. \tag{5}$$

In most cases, the term is already $\varphi^{(0)}(\eta,\,\varsigma)$ is a fairly good approximation for calculating the potential. This is due to the fact that large values of the derivative $\frac{\partial^2\varphi^{(0)}}{\partial\eta^2} = -\frac{\partial^2\varphi^{(0)}}{\partial\zeta^2}$ on the right side (5) takes in the area, where $\eta \cong 0$. In this area $\varphi^{(1)}(\eta,\,\varsigma)$ approximately satisfies the two-dimensional Laplace equation:

$$\frac{\partial^2\varphi^{(1)}}{\partial\eta^2} + \frac{\partial^2\varphi^{(1)}}{\partial\zeta^2} = 0\,, \tag{6}$$

which, under zero Dirichlet boundary conditions on a closed boundary, has an identically zero solution.

Let us consider the CMACE proposed in the work [5]. The electrode system of such an analyzer is shown schematically in Fig. 1.Here R_1, R_2 – radii of the inner and outer cylindrical surfaces, respectively, L – distance between the end electrodes. We will assume that the potentials of the ends and the inner cylinder are the same and equal V_0 , and the potential of the outer cylinder is equal to V .

The parameter R in formulas (1) is defined by the expression:

$$R = \sqrt{R_1 R_2}\,. \tag{7}$$

In variables η и ζ potential $\varphi(\zeta,\eta)$ satisfies the boundary conditions in the symmetrical rectangle shown in Fig. 2. The potential of the upper electrode, for which $\eta = \eta_k$, equal V, and the remaining electrodes have potential V_0. Quantities η_k and ζ_k in the figure are defined by the expressions:

$$\eta_k = \ln\sqrt{\frac{R_2}{R_1}}, \quad \zeta_k = \frac{L}{2R}. \tag{8}$$

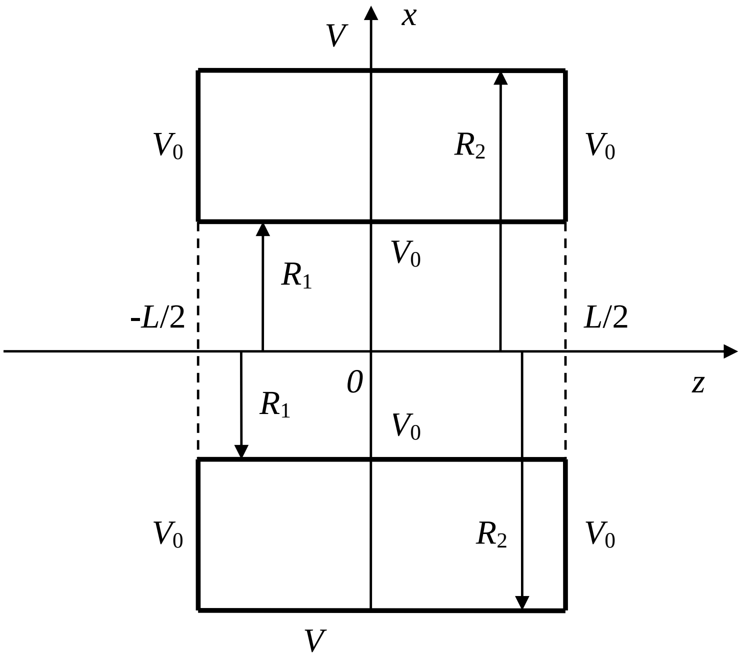

Fig. 1. Image of the projection of the electrodes of the CMACE onto the *x z* plane of the accompanying Cartesian coordinate system.

Let's map this rectangle onto the upper half-plane of the complex plane $w = u + iv$, using conformal transformation [7]:

$$\zeta + i\eta = i\eta_k + C\int_0^w \frac{dw}{\sqrt{(1-w^2)(1-\frac{w^2}{a^2})}}. \tag{9}$$

Here are the dots ± 1 w- planes correspond to vertices $\mp\zeta_k + i\eta_k$, and the points $\pm a$ – to the peaks $\mp\zeta_k - i\eta_k$ respectively. To determine the constants, the following integrals must be calculated:

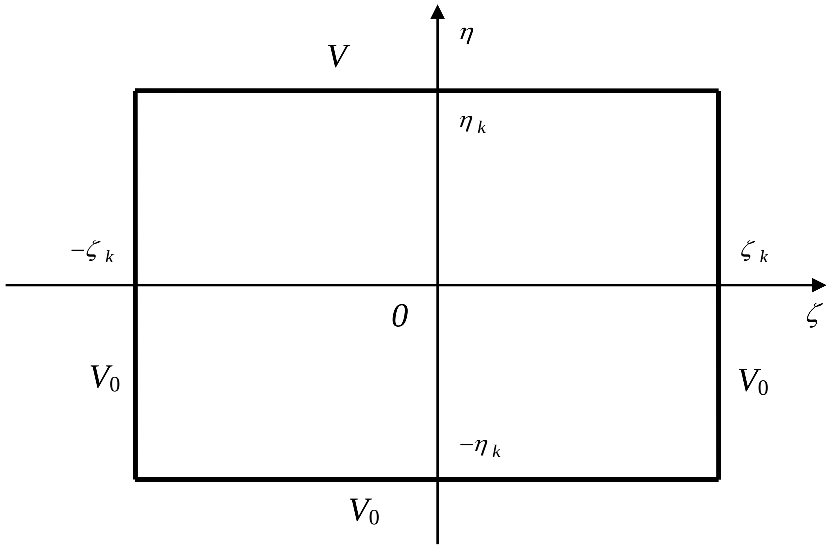

Fig. 2. Boundary value problem in the $\zeta\eta$ plane

$$C J_1 = C\int_0^1 \frac{du}{\sqrt{(1-u^2)(1-\frac{u^2}{a^2})}} = -\zeta_k, \tag{10}$$

$$-iCJ_2 = -iC\int_1^a \frac{du}{\sqrt{(u^2-1)(1-\frac{u^2}{a^2})}} = i\,2\eta_k, \tag{11}$$

Integrals J_1, J_2 in expressions (10), (11) are elliptical. Their values were found numerically, and in a small δ- neighborhoods of special points ± 1, $\pm a$ the integrals were calculated analytically, which made it possible to obtain calculation accuracy no worse than δ^2:

$$J_1 = \int_0^{1-\delta} \frac{du}{\sqrt{(1-u^2)(1-\frac{u^2}{a^2})}} + \frac{\delta}{\sqrt{2\left(1-\frac{1}{a^2}\right)}}, \tag{12}$$

$$J_2 = \int_{1+\delta}^{a-\delta} \frac{du}{\sqrt{(u^2-1)(1-\frac{u^2}{a^2})}} + \frac{\delta}{\sqrt{2\left(1-\frac{1}{a^2}\right)}} + \frac{\delta}{\sqrt{a\left(a^2-1\right)\left(1+\frac{1}{a}\right)}}, \tag{13}$$

In Table 1 for different values of the parameter a The calculated values of the integrals are given J_1, J_2, and also their ratio, equal to:

$$\frac{J_1}{J_2} = \frac{\zeta_k}{2\eta_k}. \tag{14}$$

Journal of Physics: Conference Series **2984** (2025) 012030 doi:10.1088/1742-6596/2984/1/012030

Table 1. Values of integrals J_1, J_2 depending on the value of the *a* parameter

a	J_1	J_2	J_1/J_2
1,1	2,318616	1,639984	1,413805
1,2	2,064762	1,712320	1,205827
1,5	1,807818	1,900835	0,951065
2,0	1,684159	2,153757	0,781963
3,0	1,615925	2,526283	0,639645

The calculation is carried out as follows: the geometry of the system is specified and, according to formulas (8), for the given geometry, the following are found: ζ_k and η_k then the value of the parameter a is selected in such a way that the relation (14) is satisfied and for the found value of the parameter a the constant is found from the expression (10) *C*.

Distribution of harmonic potential in the plane w is determined by the expression:

$$F^{(0)}(u,v) = V_0 + \frac{V - V_0}{\pi}\left(\operatorname{arctg}\frac{1-u}{v} + \operatorname{arctg}\frac{1+u}{v}\right). \quad (15)$$

Let us also write down the partial derivatives of the harmonic potential (15):

$$F_u^{(0)} \equiv \frac{\partial F^{(0)}}{\partial u} = \frac{V - V_0}{\pi} v \left[\frac{1}{v^2 + (1+u)^2} - \frac{1}{v^2 + (1-u)^2}\right], \quad (16)$$

$$F_v^{(0)} \equiv \frac{\partial F^{(0)}}{\partial v} = -\frac{V - V_0}{\pi}\left[\frac{1+u}{v^2 + (1+u)^2} + \frac{1-u}{v^2 + (1-u)^2}\right]. \quad (17)$$

Solving the differential equation for equipotentials:

$$\frac{dv}{du} = -\frac{F_u^{(0)}}{F_v^{(0)}}, \quad (18)$$

let's build a picture of equipotentials in the plane, w which is shown in Fig. 3. Here the electrode with potential $V = 2$ is located on the real axis in the interval $-1 < u < 1$, and on the rest of the real axis the potential $V_0 = 1$. The graph shows nine equipotentials with potential $F^{(0)}/V_0 = 1.9;1.8;...;1.1$.

To find the harmonic part of the potential $\varphi^{(0)}(\zeta,\eta)$, defining the field of the Central Zone of the Atomic Energy System, it is necessary to move from the variables in expression (15) u, v to variables ζ,η using the conformal transformation (9). Correction $\varphi^{(1)}(\zeta,\eta)$ satisfies zero boundary conditions in the rectangle shown in Fig. 2, as well as on the axes ζ, η and can be found by reducing equation (5) to a system of ordinary differential equations [6]. In what follows, we will neglect this correction due to its smallness..

Using the potential $F^{(0)}(u,v)$, it is possible to find the derivatives of the harmonic potential $\varphi^{(0)}(\zeta,\eta)$ in variables ζ,η, using the conformal transformation (9). As a result we obtain:

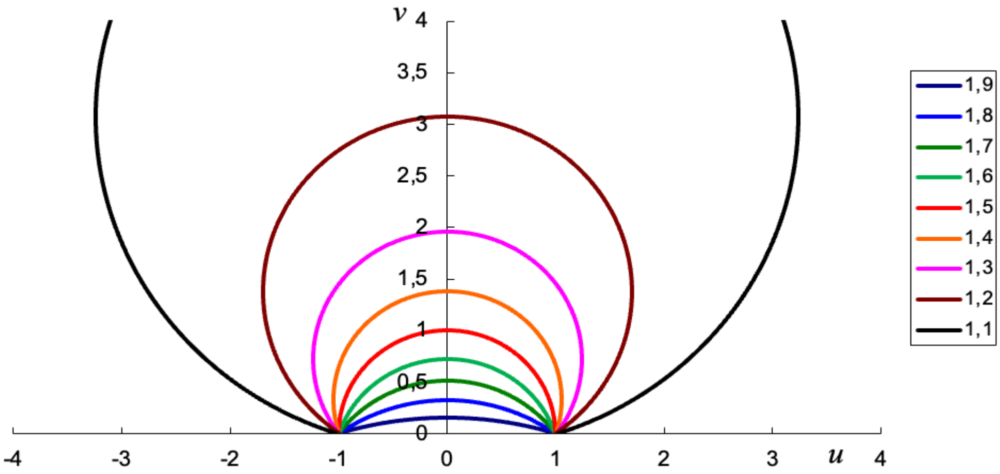

Fig. 3. Equipotential picture in the uv plane.

$$\frac{\partial\varphi^{(0)}}{\partial\zeta}=\frac{\partial F^{(0)}}{\partial u}\frac{\partial u}{\partial\zeta}+\frac{\partial F^{(0)}}{\partial v}\frac{\partial v}{\partial\zeta}, \qquad \frac{\partial\varphi^{(0)}}{\partial\eta}=\frac{\partial F^{(0)}}{\partial u}\frac{\partial u}{\partial\eta}+\frac{\partial F^{(0)}}{\partial v}\frac{\partial v}{\partial\eta}. \tag{19}$$

Differentiating (9), we write the relationship:

$$\frac{Ca}{\sqrt{(1-w^2)(a^2-w^2)}}=\frac{\partial\zeta}{\partial u}-i\frac{\partial\zeta}{\partial v}=\frac{\partial\eta}{\partial v}+i\frac{\partial\eta}{\partial u}. \tag{20}$$

Where

$$\frac{\partial\zeta}{\partial u}=\frac{\partial\eta}{\partial v}=\frac{Ca\cos\frac{\psi_1+\psi_2}{2}}{\sqrt[4]{\left[\left(1-u^2+v^2\right)^2+4u^2v^2\right]\left[\left(a^2-u^2+v^2\right)^2+4u^2v^2\right]}}. \tag{21}$$

$$-\frac{\partial\zeta}{\partial v}=\frac{\partial\eta}{\partial u}=\frac{Ca\sin\frac{\psi_1+\psi_2}{2}}{\sqrt[4]{\left[\left(1-u^2+v^2\right)^2+4u^2v^2\right]\left[\left(a^2-u^2+v^2\right)^2+4u^2v^2\right]}}. \tag{22}$$

Here

$$\psi_1=\mathrm{arctg}\frac{2uv}{1-u^2+v^2}, \qquad \psi_2=\mathrm{arctg}\frac{2uv}{a^2-u^2+v^2}. \tag{23}$$

The inverse derivatives included in (19) are found using the formulas:

Journal of Physics: Conference Series **2984** (2025) 012030 doi:10.1088/1742-6596/2984/1/012030

$$\frac{\partial u}{\partial \zeta}=\frac{\partial v}{\partial \eta}=\frac{\dfrac{\partial \zeta}{\partial u}}{\left(\dfrac{\partial \zeta}{\partial u}\right)^2+\left(\dfrac{\partial \zeta}{\partial v}\right)^2}, \quad \frac{\partial u}{\partial \eta}=-\frac{\partial v}{\partial \zeta}=-\frac{\dfrac{\partial \zeta}{\partial v}}{\left(\dfrac{\partial \zeta}{\partial u}\right)^2+\left(\dfrac{\partial \zeta}{\partial v}\right)^2}. \tag{24}$$

Equipotentials of the field in variables ζ,η can be constructed by solving equation (18) together with the equations:

$$\frac{d\zeta}{du}=\frac{\partial \zeta}{\partial u}+\frac{\partial \zeta}{\partial v}\frac{dv}{du}. \tag{25}$$

$$\frac{d\eta}{du}=\frac{\partial \eta}{\partial u}+\frac{\partial \eta}{\partial v}\frac{dv}{du}. \tag{26}$$

Picture of field equipotentials in the $\zeta\eta$ plane is shown in Fig. 4. The figure shows the calculation results for the CMACE, which $R_1=1$, $R_2=L=2$. For this system $\zeta_k=0.707107$, $\eta_k=0.346574$, $a=1,38590$, C = – 0.378137. At $V=2$, $V_0=1$ equipotential potentials vary from $1.9V_0$ to $1.1V_0$ via $0.1V_0$.

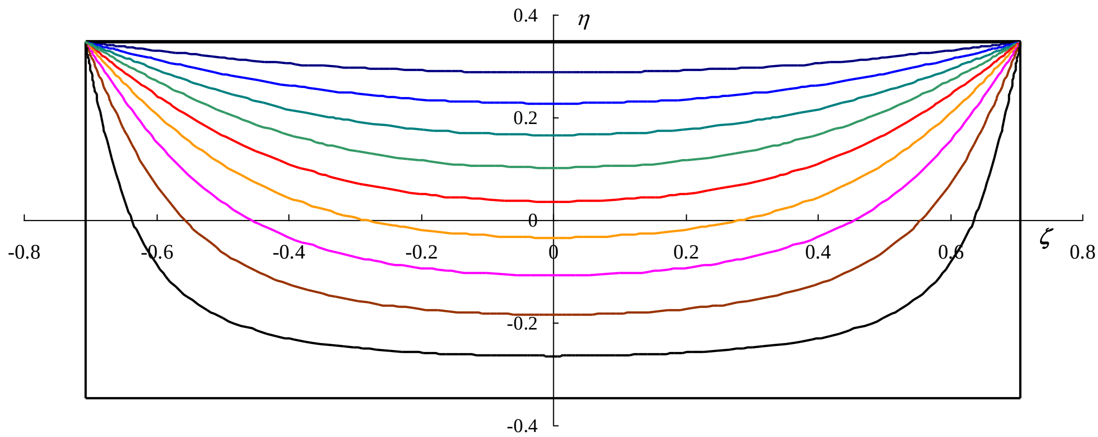

Fig. 4. Equipotential picture in the plane $\zeta\eta$ for the CMACE, which $\zeta_k=0.707107$, $\eta_k=0.346574$, $a=1.38590$, C = – 0,378137

Field picture in the xz plane for the same system is shown in Fig. 5. This figure shows the field only in the upper part of the cross-section of the cylinders, located in the region $x>0$. This figure shows that the electric field is practically absent in the lower corner points of the rectangle shown. The holes in these areas are used to input and output charged particles into the CMACE without using grids.

Journal of Physics: Conference Series **2984** (2025) 012030 doi:10.1088/1742-6596/2984/1/012030

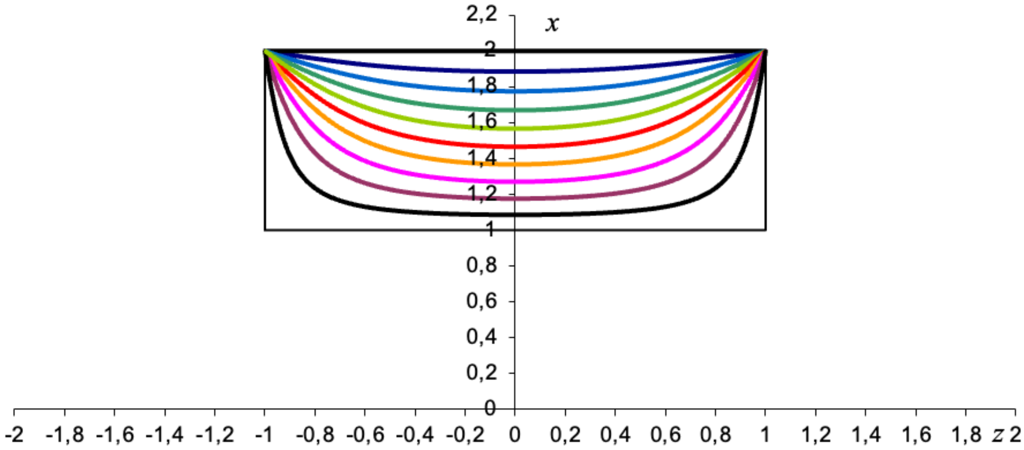

Fig. 5. Equipotential picture in the plane xz for the same CMACE

2. CALCULATION OF PARTICLE TRAJECTORIES

We will consider flat beams of charged particles from a point source located along the axis of the cylinders. Let the particles move in the plane xz axisymmetric electrostatic field. The equations of motion of a charged particle in the CMACE in dimensionless Cartesian coordinates can be written as follows:

$$\ddot{x} = -\frac{\partial \Phi}{\partial x}, \qquad \ddot{z} = -\frac{\partial \Phi}{\partial z}. \tag{27}$$

Here $\Phi = F^{(0)}/V_0$ – dimensionless potential, the unit of length is taken as the quantity *R*, defined by formula (7), the dots denote derivatives with respect to dimensionless time $\tau = t/\tau_0$, where

$$\tau_0 = R\sqrt{\frac{m}{|qV_0|}}. \tag{28}$$

In the last formula m – particle mass, q – electric charge of a particle. If the initial value $\dot{y}_0 = 0$, then the particles in the process of their movement move in the radial plane xz. In this case, the motion of particles is described by equations (27). Moreover,

$$\frac{\partial \Phi}{\partial x} = \frac{\partial \Phi}{\partial u}\frac{\partial u}{\partial \eta}\frac{\partial \eta}{\partial x} + \frac{\partial \Phi}{\partial v}\frac{\partial v}{\partial \eta}\frac{\partial \eta}{\partial x}, \tag{29}$$

$$\frac{\partial \Phi}{\partial z} = \frac{\partial \Phi}{\partial u}\frac{\partial u}{\partial \zeta}\frac{\partial \zeta}{\partial z} + \frac{\partial \Phi}{\partial v}\frac{\partial v}{\partial \zeta}\frac{\partial \zeta}{\partial z}. \tag{30}$$

In the numerical integration of equations (27), the initial conditions for the beam particles were specified on the symmetry axis: $x_0 = 0$, $z_0 = l_0$; $\dot{x}_0$, $\dot{z}_0 = 0$, at that

$\upsilon_0 = \sqrt{\dot{x}_0^2 + \dot{z}_0^2} = \sqrt{2(1+\varepsilon)}$. Here ε characterizes the relative spread of energy in the initial beam. Simultaneously with equations (27), the following equations were integrated:

$$\dot{u} = \frac{\partial u}{\partial \eta}\frac{\partial \eta}{\partial x}\dot{x} + \frac{\partial u}{\partial \zeta}\frac{\partial \zeta}{\partial z}\dot{z}, \tag{31}$$

$$\dot{v} = \frac{\partial v}{\partial \eta}\frac{\partial \eta}{\partial x}\dot{x} + \frac{\partial v}{\partial \zeta}\frac{\partial \zeta}{\partial z}\dot{z}. \tag{32}$$

The following initial conditions were given for these equations: $v_0 = 0$, $u_0 = a$. From the solution of equations (31), (32) the variables were found *u* and *v*, giving the image of the trajectory - plane. This made it possible to find the derivatives of the potential included in (27) using formulas (16), (17) and (29), (30).

The calculation of trajectories for the CMACE was carried out, which $R_1 = 1, R_2 = L = 2$. For this system $\zeta_k = 0.707107$, $\eta_k = 0.34657459$, $a = 1.385756$, C = – 0.378117. The potential of the external electrode was selected in such a way that the trajectory passed through the edge of the end electrode adjacent to the internal cylinder. This requirement corresponds to the value $V = -0.0572$ $(V_0 = 1)$. The trajectories of the monoenergetic beam calculated in this way are shown in Fig. 6. It is evident that the beam is focused near the cylinder axis. This figure also shows the axial trajectory of the beam, for which $\varepsilon = 0$, as well as trajectories that differ from the axial one with a relative deviation in energy $\varepsilon = \pm 0.1$. From these data, the linear dispersion of the analyzer along the cylinder axis is approximately equal to 6.0 per 100% energy change.

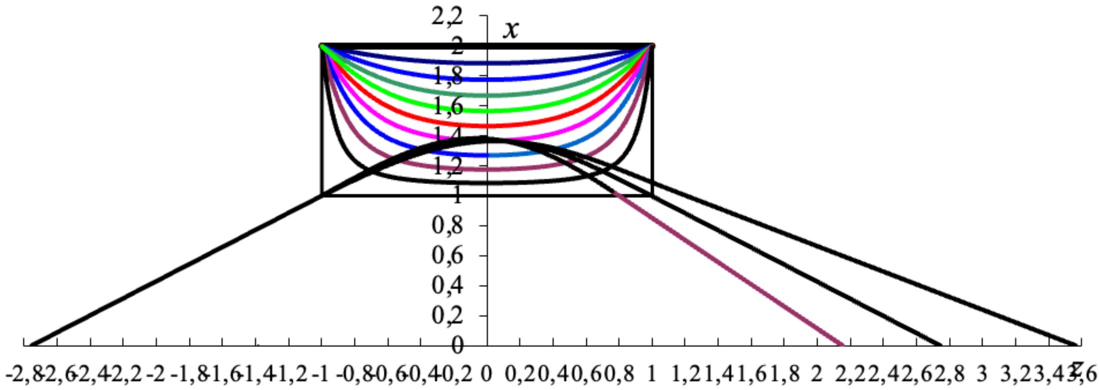

Fig. 6. Trajectories of a beam of charged particles in the CMACE, which $R_1 = 1, R_2 = L = 2$, potential at the braking electrode $V = -0{,}0572$.

Journal of Physics: Conference Series **2984** (2025) 012030 doi:10.1088/1742-6596/2984/1/012030

CONCLUSION

The paper uses a method for calculating the spatial distribution of potential in axisymmetric mirrors based on the use of CVFT methods. The field distribution in a cylindrical mirror analyzer with closed ends (CMACE) is found. CMACEs are calculated in which the beam is input and output in the analyzer through a hole in the electrodes, where the field is practically absent. Analyzer versions with high resolution and luminosity due to the rotational symmetry of the field and the presence of second-order focusing in the detector plane are found.

The authors express their gratitude to Professor E. M. Yakushev for useful discussions.

Funding

The work was carried out within the framework of a project with grant funding from the Ministry of Science and Higher Education of the Republic of Kazakhstan (AR22685992)

REFERENCES

1. V.V.Zashkvara, M.I. Korsunsky, O.S. Kosmachev Focusing action of an electrostatic mirror with a cylindrical field // J. Tech. Phys. 1966. Vol. 36, No. 1. Pp. 132-138.
2. V.P. Afanasyev, S.Ya. Yavor Electrostatic energy analyzers of charged particle beams Moscow: Nauka, 1978. – 236 p.
3. Yu.K.Golikov., N.K. Krasnova Theory of synthesis of electrostatic energy analyzers St. Petersburg: Publ. Polytechnic University, 2010. – 409 p.
4. Zh.T.Kambarova, A.O. Saulebekov, A. A. Trubitsyn The All-sky Spectrometer of Hot Cosmic Plasma // The Astronomical Journal, 164:47 (10pp), 2022 August. – https://iopscience.iop.org/article/10.3847/1538-3881/ac7561
5. L.P. Ovsyannikova, T.Ya. Fishkova Cylindrical mirror energy analyzer with closed ends // J. Tech. Phys. 1994. Vol. 64, No. 10. Pp. 174-177.
6. I.F.Spivak-Lavrov, G.A. Doskeyev., T.Zh. Tleubaeva On one method for calculating electrostatic fields with axial and transaxial symmetry // Scientific instrument making. – 2014, vol. 24, no. 1. – pp. 90-95.
7. M.A. Lavrentyev, B.V. Shabat Methods of the theory of functions of a complex variable. M.: Nauka, 1973. – 736 p.